中国激光

基于二次谐波成像定量评估主动脉增龄性改变

王楠楠[1,2,3]，高玉峰[3]，郑炜[3]，李慧[3**]，林展翼[1,2*]

[1]华南理工大学医学院，广东 广州 510006；

[2]南方医科大学附属广东省人民医院（广东省医学科学院），广东 广州 510080；

[3]中国科学院深圳先进技术研究院生物医学光学与分子影像研究中心，广东 深圳 518055

摘要 衰老是引起主动脉硬化进而引发各种心血管疾病的主要独立风险因素。对主动脉增龄性改变进行定量评估有望为心血管疾病研究提供重要线索。采用二次谐波成像技术，结合三维灰度共生矩阵纹理分析算法，对不同周龄大鼠主动脉血管壁内外表面的胶原纤维进行了定量评估；提取出多种可量化表征主动脉增龄性改变的特征参数，从胶原纤维微结构角度揭示了主动脉增龄性变化规律。上述方法及提取出的特征参数有望为评估血管老化程度提供有力工具和重要参考指标，并进一步应用于与老化相关的心血管疾病的研究。

关键词 医用光学；二次谐波成像；三维灰度共生矩阵；主动脉；增龄性改变；胶原纤维

中图分类号 Q631 **文献标志码** A **DOI**：10.3788/CJL221414

1 引 言

心血管疾病在中国城乡居民死亡原因中居首位[1]。心血管系统在疾病发生发展过程中的结构与功能变化一直是心血管界研究的重要课题之一。主动脉作为连接心脏与外周组织的重要通道，需要具有较好的弹性，以便在心脏收缩时吸收血流动能缓冲收缩压，在心脏舒张时释放势能调节舒张压[2-3]。衰老会降低主动脉的弹性，导致血管逐渐硬化（又称“血管重塑”）[4]。该过程通常会伴随着血压升高，并进一步引发多种心血管疾病，包括主动脉瘤[5]、主动脉夹层[6]及动脉粥样硬化[7]等。动脉壁良好的弹性性能与其细胞外基质中富含的纤维蛋白密切相关，纤维组织的三维各向异性结构对于血管功能的实现至关重要[8]。胶原纤维是主要的纤维蛋白，是支撑主动脉力学性能和弹性的核心物质之一[9]。因此，研究主动脉壁胶原纤维的增龄性改变，对于进一步揭示心血管疾病的发生发展具有重要意义。

目前，二次谐波（SHG）显微成像技术已经成为观测生物组织内胶原纤维微结构的理想工具[10-11]。相比于传统的组织切片染色观测方法，SHG成像无须对组织进行标记、切片即可利用胶原纤维有序且非中心对称的结构特点对其进行高分辨、特异性观测，并且天然具有层析能力、低光漂白和光毒性、深组织穿透能力等独特优势[12-13]。目前，SHG技术已被应用于血管老化[14]、动脉粥样硬化[15-16]、主动脉瘤[17-18]、马方综合征[19-20]等与心血管疾病相关的生理、病理研究中；然而，这些研究大多局限于对胶原纤维的定性[21]或二维定量评估[22-24]，通常带有一定的主观性和片面性，准确性和可重复性难以保证。三维灰度共生矩阵（3D GLCM）是最具代表性的空间纹理分析算法之一，该算法通过量化三维图像内不同体素灰度值之间的相互关系，从多个角度定量表征图像的三维纹理特征[25]，具有强大的图像分析能力，在生物医学研究中一直发挥着重要作用[26]。然而，目前该方法在表征心血管纤维微结构方面的应用仅限于动脉粥样硬化斑块的识别研究，在探索血管壁增龄性改变上的潜力还有待评估。

笔者采用SHG显微成像技术，对不同周龄大鼠主动脉血管壁内外表面的胶原纤维进行了三维无标记成像，结合3D GLCM算法提取出了多种可量化表征主动脉血管壁胶原纤维增龄性改变的空间纹理特征，并从胶原纤维微结构角度揭示主动脉增龄性变化的规律。这一方法以及所提取的关键纹理特征参数，有望被进一步应用于与心血管老化相关的疾病的发病机制研究中。

2 材料和方法

2.1 样本制备

本次实验采用北京维通利华实验动物技术有限公司的Wistar-Kyoto（WKY）大鼠作为实验对象，其周龄

收稿日期：2022-11-14；**修回日期**：2023-01-09；**录用日期**：2023-03-06；**网络首发日期**：2023-03-16

基金项目：国家自然科学基金（92159104，82071972）、深圳市科技计划基础研究项目（RCYX20210609104445093，RCJC20200714114433058，ZDSY20130401165820357）

通信作者：*linzhanyi@gdph.org.cn；**hui.li@siat.ac.cn

涵盖三个阶段：3周龄（3 w），4只；12周龄（12 w），4只；44周龄（44 w），3只。这三个周龄分别对应于大鼠的幼龄期、成年早期和成年晚期，是研究大鼠增龄性改变比较典型的年龄阶段。WKY大鼠饲养于无特定病原体级的动物房内，按照国际标准喂养。本研究所涉及的所有动物实验已获得中国科学院深圳先进技术研究院实验动物管理和使用委员会的许可。具体实验步骤如下：先使用CO_2安乐死箱对WKY大鼠进行处死，并从其体内摘取主动脉的腹腔部分；然后将摘取的组织用磷酸缓冲盐溶液冲洗3 min，去除血管腔内的血液；最后将血管外膜表面的脂肪组织剪除干净，再沿血管壁轴向将血管剪开，分别将血管内表面和外表面向上平铺在载玻片上，盖上盖玻片，在显微镜下成像。

2.2 成像设备

采用商业多光子显微成像系统（A1R-MP）对WKY大鼠主动脉进行SHG成像，获取其血管壁内外表面胶原纤维的微结构信息。该成像系统以钛蓝宝石激光器（MaiTai eHP DeepSee，Spectra Physics）作为激发光源，激发波长设置为790 nm。在该激发波长下，分别对大鼠动脉壁的内（内膜和中膜）、外（外膜）表面进行三维成像，两者相结合的成像深度能够覆盖整个动脉壁的厚度（三个年龄段相比，44 w大鼠的动脉壁是最厚的，基于其横截面的H&E染色切片图像测得内膜和中膜厚度之和约为60～90 μm，外膜厚度约为60～90 μm，而内外表面成像深度均可达到100 μm以上）。物镜（N25X-APO-MP，Nikon）采用25×、数值孔径NA=1.1的水镜。在探测端使用395 nm/25 nm窄带滤光片（ET395/25m-2p，Chroma）分离出SHG信号（对应的最佳激发波长为790 nm）。成像视场尺寸为520 μm×520 μm。系统的理论横向、纵向分辨率分别约为277、850 nm。为了能够在揭示胶原纤维精细纹理结构以及保证足够大成像视场的前提下，避免长时间成像对样品造成光漂白和光损伤，采用0.51 μm/pixel的横向分辨率和3 μm/pixel的纵向分辨率进行采样。

2.3 3D GLCM分析

本研究采用3D GLCM分析WKY大鼠主动脉胶原纤维的纹理特征。对于一个三维图像，设其灰度级为g，则灰度值分别为i和j（$0\leqslant i<g$，$0\leqslant j<g$）且空间位置关系由矢量$\boldsymbol{d}$定义的一对体素（3D空间中的像素）在图像中出现的概率构成了二阶联合分布概率$p(i,j|\boldsymbol{d},g)$。$\boldsymbol{d}$可以用距离$|\boldsymbol{d}|$和方向(α,β)两个要素来表征，其中α为方位角，β为极角，如图1所示。基于$p(i,j|\boldsymbol{d},g)$，笔者主要提取出了6个纹理特征参数，分别为相关性（C）、对比度（C_t）、熵（E）、和均值（S_m）、方差（V）、同质性（H），它们分别表征纤维纹理的一致性、清晰度、强度非均质性、总体强度、强度集中性、结构各向同性。这些特征参数的具体定义为

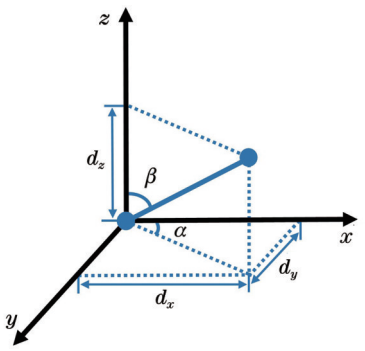

图1 3D GLCM方法中决定一对体素（蓝色点）之间相对位置的参数

Fig. 1 Definitions of parameters that determining the relative position between a pair of voxels (blue dots) in 3D GLCM

$$C=\frac{\sum_{i=0}^{g-1}\sum_{j=0}^{g-1}(ij)\cdot p(i,j)-\mu_x\mu_y}{\sigma_x\sigma_y},\tag{1}$$

$$C_t=\sum_{k=0}^{g-1}\left(|i-j|\right)^2\left\{\sum_{i=0}^{g-1}\sum_{j=0}^{g-1}p(i,j)\right\},\tag{2}$$

$$E=-\sum_{i=0}^{g-1}\sum_{j=0}^{g-1}p(i,j)\lg\left[p(i,j)\right],\tag{3}$$

$$S_m=\sum_{i=0}^{g-1}\sum_{j=0}^{g-1}(i+j)\,p(i,j),\tag{4}$$

$$V=\sum_{i=0}^{g-1}\sum_{j=0}^{g-1}(i-\mu_x)^2\cdot p(i,j)+\sum_{i=0}^{g-1}\sum_{j=0}^{g-1}(j-\mu_y)^2\cdot p(i,j),\tag{5}$$

$$H=\sum_{i=0}^{g-1}\sum_{j=0}^{g-1}\frac{1}{1+(i-j)^2}p(i,j),\tag{6}$$

式中：μ_x、μ_y分别为3D GLCM中行和列的均值；σ_x、σ_y分别为3D GLCM中行和列的标准偏差值[27]。在本研究中，3D GLCM分析涉及$|\boldsymbol{d}|$=3，4，5，6共4个距离以及(α,β)=(-，0°)，(0°，45°)，(45°，45°)，(90°，45°)，(135°，45°)，(0°，90°)，(45°，90°)，(90°，90°)，(135°，90°)，(0°，135°)，(45°，135°)，(90°，135°)，(135°，135°)共13个三维方向。最终用于统计、分析和对比的纹理特征值通过对不同距离和角度下的计算结果进行平均得到。上述计算使用MATLAB（MathWorks）完成。

需要强调的是，在进行3D GLCM分析之前，先对原始图像进行了直方图均衡化处理，目的是使3D GLCM特征参数值几乎不受原始图像强度差异的影响，确保其仅反映胶原纤维的纹理特征。此外，大鼠血管壁的厚度会随着周龄增加而逐渐增加，其中变化最显著的阶段是从出生到成熟的两个月内[28]。因此，为了保证对比的公平性（即血管内表面都只取内膜和中膜的图像进行分析，而外表面仅提取外膜图像进行分析），3 w大鼠主动脉血管内外表面各取30 μm深度范围内的图像，而12 w和44 w的WKY大鼠则取60 μm深度范围内的图像用于后续的定量分析。

2.4 统计分析

采用GraphPad Prism软件（V9.0，GraphPad

Software)对3D GLCM特征参数值进行统计分析,采用单因素方差分析(One-way ANOVA)对不同年龄组的数据进行比较,$P<0.05$表示具有显著性差异。

3 结果和讨论

3.1 大鼠主动脉胶原纤维的三维SHG图像

为了揭示WKY大鼠主动脉胶原纤维随周龄增长的变化规律,采用SHG显微成像技术对不同周龄(3 w、12 w、44 w)WKY大鼠主动脉内表面(内膜、中膜)和外表面(外膜)的胶原纤维进行三维成像,成像结果如图2和图3所示。从图2中可以看出大鼠在生长和成熟老化过程中,血管内膜、中膜胶原纤维发生了一系列的形态结构变化:3 w大鼠主动脉胶原纤维较细,排列得相对紧密且分布较为不均匀;12 w和44 w大鼠主动脉胶原纤维明显变粗,排列得相对疏松且分布更加均匀。

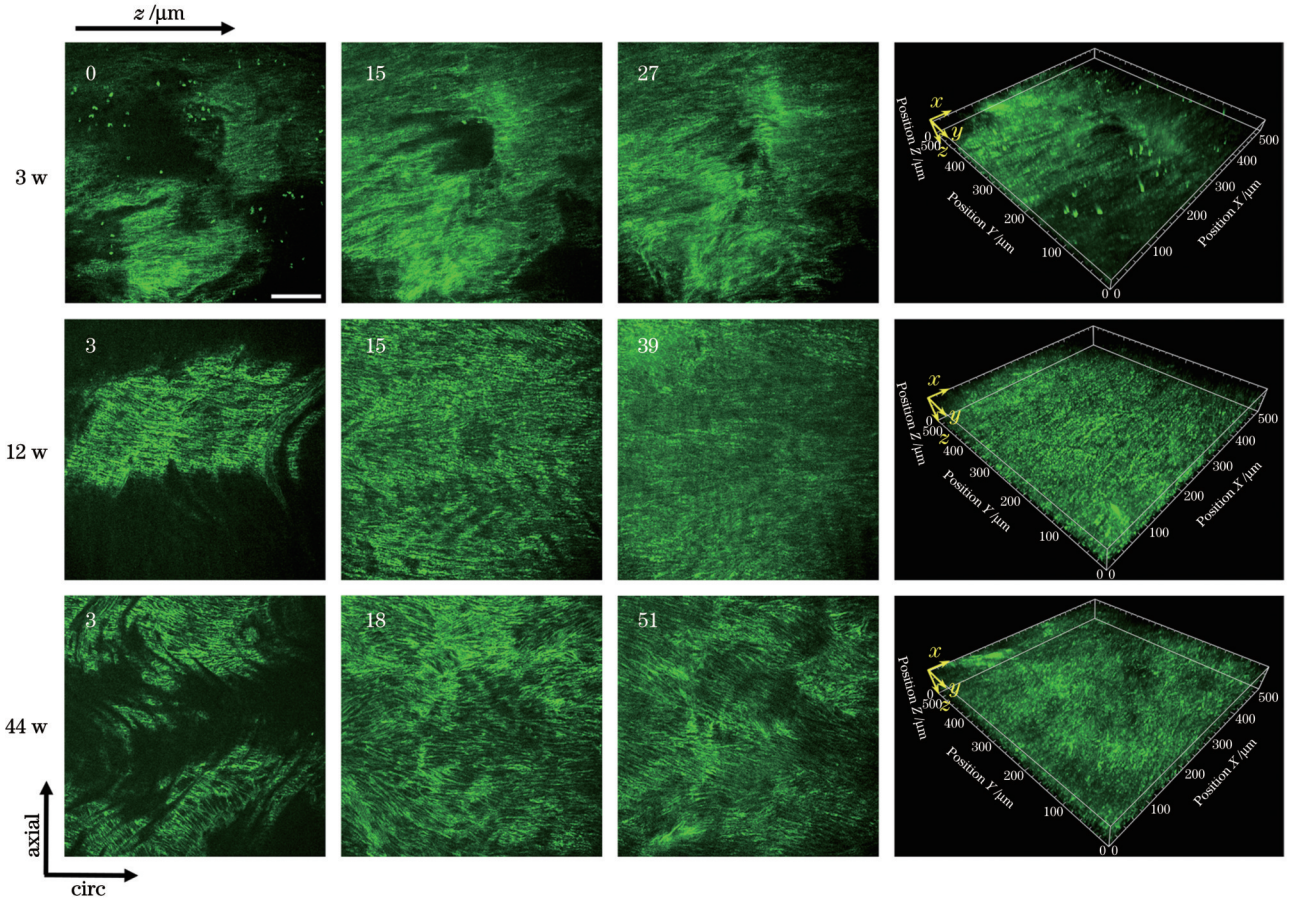

图2 不同周龄组大鼠主动脉内膜和中膜胶原纤维的3D SHG图像(前3列是距离血管内表面不同深度处胶原纤维的二维图像,左上角数字表示深度值;第4列为三维重建图像。标尺:100 μm)

Fig. 2 3D SHG images of collagen fibers within aortic intima and media of rats with different weeks of age (The left three columns show 2D images of collagen fibers at different depths from the inner surface of the vascular and the upper left digit indicates the depth value. The fourth column is the 3D reconstructed image. Scale bar: 100 μm)

主动脉血管壁外膜胶原纤维增龄性改变的规律与内膜、中膜胶原纤维增龄性改变的规律具有一定的一致性,即:从3 w到12 w、44 w,胶原纤维的分布变得疏松且均匀,如图3所示。但是,不同于内膜、中膜胶原纤维相互独立且细直的形态特征,外膜胶原纤维密集成束,呈现出明显的波纹状且具有更强的SHG信号。此外,相对于3 w和12 w大鼠,44 w大鼠主动脉外膜胶原纤维束在距离外表面较深处(大约45 μm处)明显变得更直。这一特征与人浅股动脉[14]及小鼠主动脉[21]的增龄性改变、人主动脉瘤[17]的病理性改变,以及猪主动脉在弹性蛋白酶处理前后[22,29]的改变类似。该变化可能与老化或病变引起弹性蛋白降解、碎裂,进而导致血管内承载力向胶原纤维发生转移[30]有关。

这些结果表明,利用SHG成像技术可以在无须对组织样本进行标记和切片的条件下,实现对主动脉血管壁胶原纤维的高分辨、特异性成像,因而有望成为评估主动脉增龄性变化的重要工具之一。

3.2 可量化表征胶原纤维增龄性改变的3D GLCM特征参数

为了进一步详细探究不同周龄WKY大鼠血管壁胶原纤维结构的差异,采用3D GLCM算法对主动脉内(内膜和中膜)、外表面(外膜)的SHG图像进行定量分析,共计算了11个特征参数,包括能量、熵、同质性、

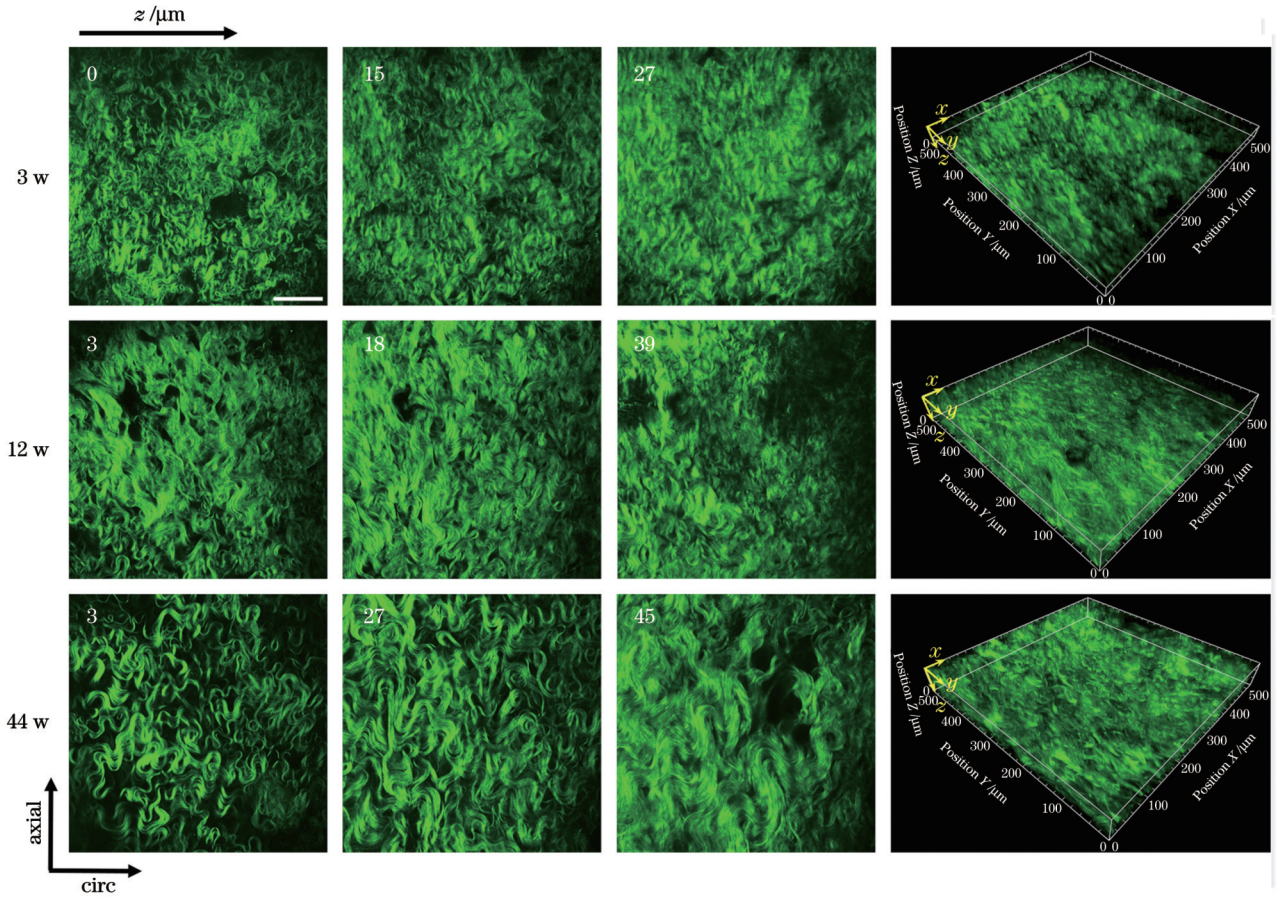

图 3　不同周龄组大鼠主动脉外膜胶原纤维的 3D SHG 图像(前 3 列为距离血管外表面不同深度处的胶原纤维的二维图像,左上角数字表示深度值;第 4 列为三维重建图像。标尺:100 μm)

Fig. 3　3D SHG images of collagen fibers within aortic adventitia of rats with different weeks of age (The left three columns show 2D images of collagen fibers at different depths from the outer surface of the vascular and the upper left digit indicates the depth value. The fourth column is the 3D reconstructed image. Scale bar: 100 μm)

对比度、方差、相关性、和均值、群聚阴暗度、群聚突出度、最大概率和逆方差。利用单因素方差分析结合 Tukey 多重比较检验方法,对上述特征参数在不同周龄组之间的差异进行统计分析。结果显示:就内表面而言,相关性、对比度、熵、和均值、方差、同质性等 6 个特征参数在不同周龄组间表现出了显著性差异,这些参数分别表征纤维纹理的一致性、清晰度、强度非均质性、总体强度、强度集中性、结构各向同性,如图 4 所示;就外表面而言,仅和均值、方差、同质性表现出显著性差异,如图 5 所示。

具体来讲,3 w 大鼠血管内表面胶原纤维与其他两个周龄组相比具有较高的相关性和较低的对比度值,这与 3 w 大鼠血管壁内表面胶原纤维的分布比较集中进而导致局部灰度值较为接近的特征相符合,如图 4(a)~(b)所示。44 w 大鼠与 3 w、12 w 大鼠的分析结果相比具有较低的熵、和均值、方差值,如图 4(c)~(e)所示,这些参数反映了生长、老化过程中主动脉内表面胶原纤维的整体分布趋于均匀。相较于其他两个周龄组,12 w 大鼠血管内表面胶原纤维的同质性较低,如图 4(f)所示,表明该周龄组血管壁内表面不同深度处的胶原纤维在信号强度上差别较大。

就主动脉外膜胶原纤维而言,相较于 12 w 和 44 w 大鼠,3 w 大鼠具有较低的同质性值[如图 5(a)所示],这符合其纤维束空间排列杂乱、不同区域间灰度值变化较大的特征。与内表面纤维结构的变化类似,3 w 大鼠和 44 w 大鼠血管外表面纤维结构的和均值、方差这两个特征参数具有显著性差异[如图 5(b)~(c)所示],反映了胶原纤维束在大鼠生长过程中具有逐渐变粗、排列变得规律且疏松、不同区域的灰度值分布趋于均匀等特征。

上述 3D GLCM 分析和统计结果表明:用 3D GLCM 结合 SHG 技术来评估大鼠血管壁内外表面胶原纤维的增龄性变化具有可行性;相关性、对比度、熵、和均值、方差、同质性这 6 个特征参数能够反映主动脉增龄性改变,尤其是同质性、和均值、方差这 3 个特征参数在内外表面胶原纤维的增龄性变化中都表现出显著性差异,有望作为判定主动脉血管老化程度的定量指标。

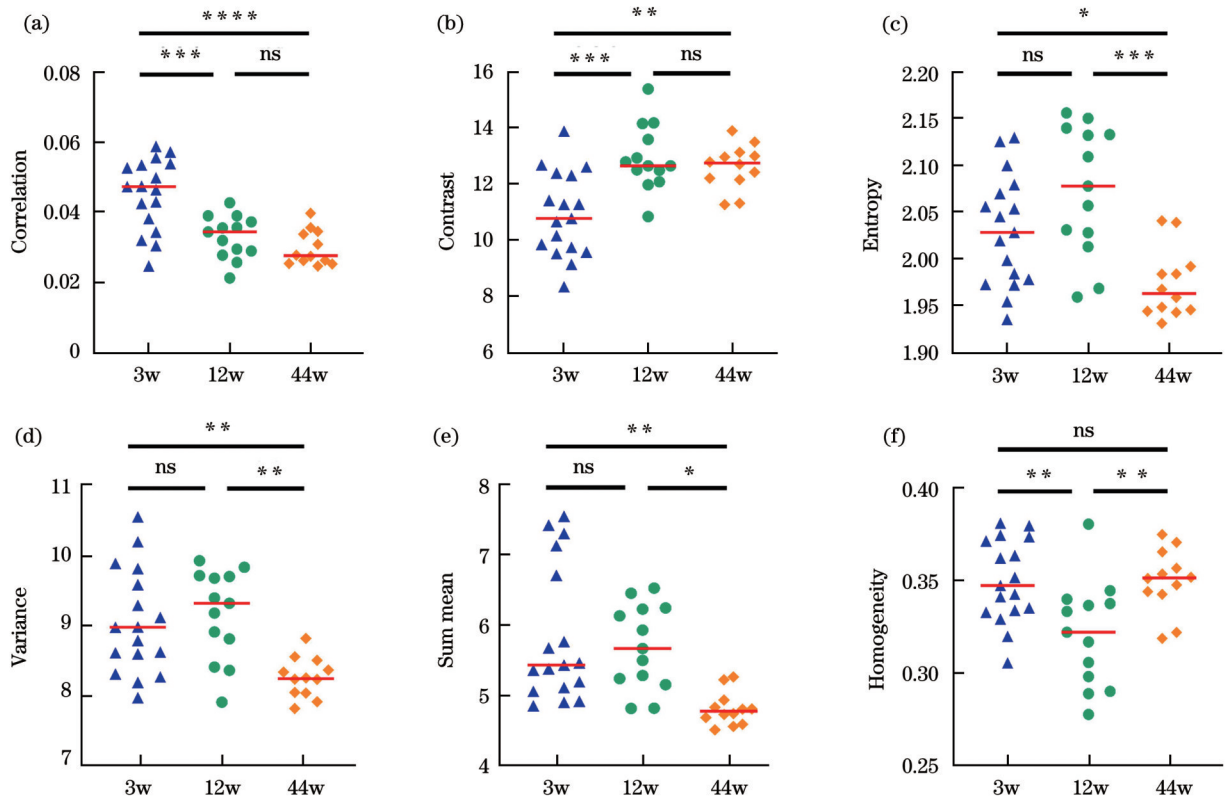

图 4 主动脉内膜、中膜胶原纤维 SHG 图像在不同周龄大鼠之间存在显著性差异的 3D GLCM 特征参数(红色实线代表中值。ns 表示无显著性差异,*表示 $0.01<P<0.05$,**表示 $0.001<P<0.01$,***表示 $0.0001<P<0.001$,****表示 $P<0.0001$,单因素方差分析结合 Tukey 多重比较检验)。(a)相关性;(b)对比度;(c)熵;(d)方差;(e)和均值;(f)同质性

Fig. 4 3D GLCM texture feature parameters derived from SHG images of aortic intima and media collagen fibers, which show significant differences among rats with different weeks of age (The red solid line indicates the median. "ns" denotes no significance, *: $0.01<P<0.05$, **: $0.001<P<0.01$, ***: $0.0001<P<0.001$, ****: $P<0.0001$, one-way ANOVA and Tukey's multiple comparison test). (a) Correlation; (b) contrast; (c) entropy; (d) variance; (e) sum mean; (f) homogeneity

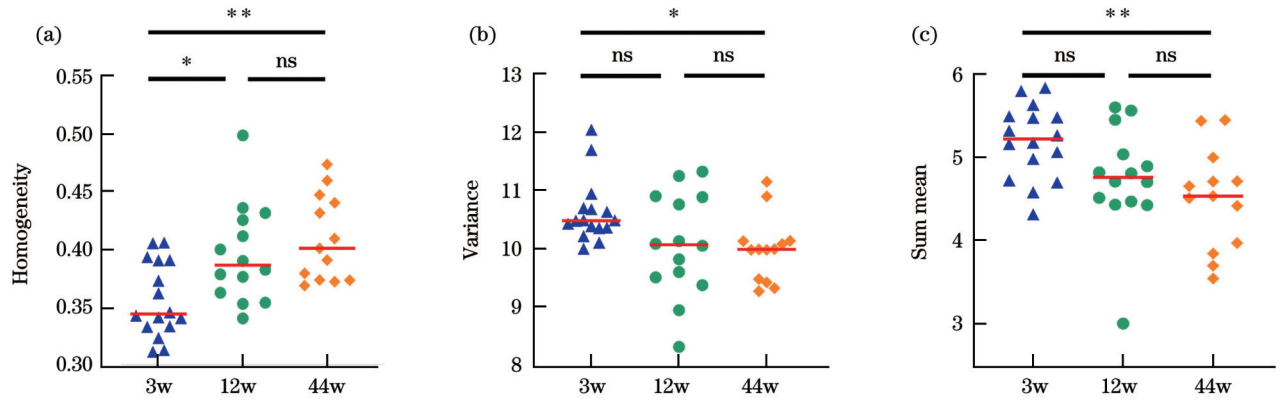

图 5 主动脉外膜胶原纤维 SHG 图像在不同周龄大鼠之间存在显著性差异的 3D GLCM 特征参数(红色实线代表中值。*表示 $0.01<P<0.05$,**表示 $0.001<P<0.01$,单因素方差分析结合 Tukey 多重比较检验)。(a)同质性;(b)方差;(c)和均值

Fig. 5 3D GLCM texture feature parameters derived from SHG images of aortic adventitia collagen fibers, which show significant differences among rats with different weeks of age (The red solid line indicates the median. *: $0.01<P<0.05$, **: $0.001<P<0.01$, one-way ANOVA and Tukey's multiple comparison test). (a) Homogeneity; (b) variance; (c) sum mean

4 结 论

使用 SHG 成像技术对不同周龄 WKY 大鼠主动脉血管壁内外表面的胶原纤维进行了三维无标记成像,并结合 3D GLCM 算法提取出一系列特征参数,以定量评估主动脉胶原纤维的增龄性改变。结果表明:相关性、对比度、熵、和均值、方差和同质性这 6 个特征参数能够用于揭示主动脉胶原纤维结构的增龄性变化规律。因此,SHG 成像技术结合 3D GLCM 算法以及所提取的特征参数,有望为研究与老化相关的心血管

疾病提供有力工具。值得一提的是，SHG成像与激发光的偏振态、偏振方向息息相关。圆偏振光可以均匀地激发所有取向的胶原纤维，而线偏振光的偏振方向会影响胶原纤维SHG信号的强度。当线偏振激发光的偏振方向与胶原纤维的取向平行时，SHG信号最强；当两者垂直时，SHG信号最弱[13]。本研究中采用的激发光源为线偏振光。虽然通过三维成像、多区域成像、统计分析以及对原始图像进行直方图均衡化处理等，最大限度地削弱了激发光偏振方向对本研究定量分析结果的影响，但仍希望未来能将偏振这一重要因素考虑进来，进一步展开深入研究。另外，3D GLCM算法对于血管壁纤维微结构的改变虽然已具有很高的敏感性，但尚无法仅凭单一特征参数彻底区分3 w、12 w、44 w这三个年龄阶段大鼠的动脉壁，未来笔者还将进一步探索更加灵敏的定量分析方法。此外，目前SHG成像受限于穿透深度及庞大的系统构架，只适用于离体组织或活体浅表组织成像。未来结合内窥成像等技术手段，有望将该方法推广到心血管系统的活体成像，最终应用于心血管疾病的临床诊断。

备注：本文支持材料可扫下方二维码获得。

参 考 文 献

[1] 国家心血管病中心. 中国心血管健康与疾病报告2020[J]. 心肺血管病杂志, 2021, 40(9): 1007-5062.
National Center for Cardiovascular Diseases. Annual report on cardiovascular health and diseases in China 2020[J]. Journal of Cardiovascular and Pulmonary Diseases, 2021, 40(9): 1007-5062.

[2] 罗华, 黄达, 蔡维君, 等. 小鼠胸主动脉壁内弹性纤维和胶原纤维的发育规律[J]. 中国组织化学与细胞化学杂志, 2020, 29(1): 34-40.
Luo H, Huang D, Cai W J, et al. Developmental pattern of elastic and collagen fibers in the thoracic aorta wall of mice[J]. Chinese Journal of Histochemistry and Cytochemistry, 2020, 29(1): 34-40.

[3] Rooprai J, Boodhwani M, Beauchesne L, et al. Thoracic aortic aneurysm growth in bicuspid aortic valve patients: role of aortic stiffness and pulsatile hemodynamics[J]. Journal of the American Heart Association, 2019, 8(8): e010885.

[4] Albu M, Şeicaru D A, Pleşea R M, et al. Assessment of the aortic wall histological changes with ageing[J]. Romanian Journal of Morphology and Embryology, 2021, 62(1): 85-100.

[5] Yang C, Kohnken R. Age-related changes in the canine aorta[J]. Veterinary Pathology, 2021, 58(2): 376-383.

[6] Davies R R, Goldstein L J, Coady M A, et al. Yearly rupture or dissection rates for thoracic aortic aneurysms: simple prediction based on size[J]. The Annals of Thoracic Surgery, 2002, 73(1): 17-28.

[7] Cicchi R, Baria E, Matthäus C, et al. Non-linear imaging and characterization of atherosclerotic arterial tissue using combined SHG and FLIM microscopy[J]. Journal of Biophotonics, 2015, 8(4): 347-356.

[8] Mammoto A, Matus K, Mammoto T. Extracellular matrix in aging aorta[J]. Frontiers in Cell and Developmental Biology, 2022, 10: 822561.

[9] Poole J J A, Mostaço-Guidolin L B. Optical microscopy and the extracellular matrix structure: a review[J]. Cells, 2021, 10(7): 1760.

[10] 张子一, 王明雪, 刘志贺, 等. 二次谐波在生物医学成像中的应用[J]. 中国激光, 2020, 47(2): 0207008.
Zhang Z Y, Wang M X, Liu Z H, et al. Application of second harmonic generation in biomedical imaging[J]. Chinese Journal of Lasers, 2020, 47(2): 0207008.

[11] Borile G, Sandrin D, Filippi A, et al. Label-free multiphoton microscopy: much more than fancy images[J]. International Journal of Molecular Sciences, 2021, 22(5): 2657.

[12] 徐顺武, 何佳佳, 席刚琴, 等. 多光子显微技术在乳腺肿瘤微环境预后预测研究中的应用进展[J]. 激光与光电子学进展, 2022, 59(6): 0617013.
Xu S W, He J J, Xi G Q, et al. Application progress of multiphoton microscopy in prognostic prediction of breast tumor microenvironments[J]. Laser & Optoelectronics Progress, 2022, 59(6): 0617013.

[13] Chen X Y, Nadiarynkh O, Plotnikov S, et al. Second harmonic generation microscopy for quantitative analysis of collagen fibrillar structure[J]. Nature Protocols, 2012, 7(4): 654-669.

[14] Jadidi M, Sherifova S, Sommer G, et al. Constitutive modeling using structural information on collagen fiber direction and dispersion in human superficial femoral artery specimens of different ages[J]. Acta Biomaterialia, 2021, 121: 461-474.

[15] 张荣丽, 李慧, 吴岳恒, 等. 利用光谱和时间分辨的多光子显微技术识别人体冠状动脉粥样硬化斑块[J]. 中国激光, 2020, 47(2): 0207025.
Zhang R L, Li H, Wu Y H, et al. Identification of human coronary atherosclerotic plaques using spectrum- and time-resolved multiphoton microscopy[J]. Chinese Journal of Lasers, 2020, 47(2): 0207025.

[16] Zhang R L, Xu Z B, Hao J H, et al. Label-free identification of human coronary atherosclerotic plaque based on a three-dimensional quantitative assessment of multiphoton microscopy images[J]. Biomedical Optics Express, 2021, 12(5): 2979-2995.

[17] Niestrawska J A, Viertler C, Regitnig P, et al. Microstructure and mechanics of healthy and aneurysmatic abdominal aortas: experimental analysis and modelling[J]. Journal of the Royal Society Interface, 2016, 13(124): 0620.

[18] Haskett D, Speicher E, Fouts M, et al. The effects of angiotensin II on the coupled microstructural and biomechanical response of C57BL/6 mouse aorta[J]. Journal of Biomechanics, 2012, 45(5): 772-779.

[19] Cui J Z, Tehrani A Y, Jett K A, et al. Quantification of aortic and cutaneous elastin and collagen morphology in Marfan syndrome by multiphoton microscopy[J]. Journal of Structural Biology, 2014, 187(3): 242-253.

[20] López-Guimet J, Andilla J, Loza-Alvarez P, et al. High-resolution morphological approach to analyse elastic laminae injuries of the ascending aorta in a murine model of Marfan syndrome[J]. Scientific Reports, 2017, 7(1): 1-13.

[21] Cavinato C, Murtada S I, Rojas A, et al. Evolving structure-function relations during aortic maturation and aging revealed by multiphoton microscopy[J]. Mechanisms of Ageing and Development, 2021, 196: 111471.

[22] Chow M J, Turcotte R, Lin C P, et al. Arterial extracellular matrix: a mechanobiological study of the contributions and interactions of elastin and collagen[J]. Biophysical Journal, 2014,

106(12): 2684-2692.
[23] Sugita S, Matsumoto T. Multiphoton microscopy observations of 3D elastin and collagen fiber microstructure changes during pressurization in aortic media[J]. Biomechanics and Modeling in Mechanobiology, 2017, 16(3): 763-773.
[24] Baria E, Nesi G, Santi R, et al. Improved label-free diagnostics and pathological assessment of atherosclerotic plaques through nonlinear microscopy[J]. Journal of Biophotonics, 2018, 11(11): e201800106.
[25] Hu W Y, Li H, Wang C Y, et al. Characterization of collagen fibers by means of texture analysis of second harmonic generation images using orientation-dependent gray level co-occurrence matrix method[J]. Journal of Biomedical Optics, 2012, 17(2): 026007.
[26] Hu Y F, Liang Z R, Song B W, et al. Texture feature extraction and analysis for polyp differentiation via computed tomography colonography[J]. IEEE Transactions on Medical Imaging, 2016, 35(6): 1522-1531.
[27] Chen W J, Giger M L, Li H, et al. Volumetric texture analysis of breast lesions on contrast-enhanced magnetic resonance images[J]. Magnetic Resonance in Medicine, 2007, 58(3): 562-571.
[28] Fornieri C, Quaglino D, Jr, Mori G. Role of the extracellular matrix in age-related modifications of the rat aorta. Ultrastructural, morphometric, and enzymatic evaluations[J]. Arteriosclerosis and Thrombosis, 1992, 12(9): 1008-1016.
[29] Zeinali-Davarani S, Chow M J, Turcotte R, et al. Characterization of biaxial mechanical behavior of porcine aorta under gradual elastin degradation[J]. Annals of Biomedical Engineering, 2013, 41(7): 1528-1538.
[30] Tsamis A, Krawiec J T, Vorp D A. Elastin and collagen fibre microstructure of the human aorta in ageing and disease: a review [J]. Journal of the Royal Society Interface, 2013, 10(83): 20121004.

Quantitative Assessment of Age-Related Changes in Aorta Based on Second Harmonic Generation Microscopy

Wang Nannan[1,2,3], Gao Yufeng[3], Zheng Wei[3], Li Hui[3**], Lin Zhanyi[1,2*]

[1]*School of Medicine, South China University of Technology, Guangzhou* 510006, *Guangdong, China*;
[2]*Guangdong Provincial People's Hospital (Guangdong Academy of Medical Sciences), Southern Medical University, Guangzhou* 510080, *Guangdong, China*;
[3]*Research Center for Biomedical Optics and Molecular Imaging, Shenzhen Institute of Advanced Technology, Chinese Academy of Sciences, Shenzhen* 518055, *Guangdong, China*

Abstract

Objective Aging is a major independent risk factor for aortic stiffness and cardiovascular diseases. The strength of the aorta is imparted by collagen fibers, which are the dominant fibrins within the aortic wall. Therefore, a three-dimensional (3D) quantitative assessment of age-related changes in the collagen fibers within the aortic wall is expected to provide important clues for research on cardiovascular diseases. Second harmonic generation (SHG) microscopy is an ideal tool for observing collagen fibers in biological tissues. Compared to the traditional histological analysis method, which requires tissue sectioning and staining, SHG microscopy has an intrinsic optical sectioning ability for the 3D imaging of intact tissues and allows label-free and high-specificity imaging of collagen fibers owing to its inversion-asymmetric and spatially ordered structure. Moreover, the high resolution, large depth penetration, low photobleaching and phototoxicity of SHG microscopy have significantly benefited the detailed imaging of thick tissues such as the aortic wall. However, the SHG-based 3D quantitative assessment of aortic collagen fibers has not yet been extensively demonstrated in aging-related research. In this study, we proposed combining SHG imaging with a representative spatial texture analysis algorithm, a 3D gray-level co-occurrence matrix (GLCM), to investigate age-related changes in the aorta from the perspective of collagen fiber microstructures. We hope that the proposed method and our findings can provide novel strategies and potential indicators for aortic aging assessment, and further benefit studies on age-related cardiovascular diseases.

Methods Wistar-Kyoto (WKY) rats at 3 weeks (3 w), 12 weeks (12 w), and 44 weeks (44 w) were used in this study. First, the abdominal aortas were removed, cleaned, and cut open along the longitudinal axis. Subsequently, en-face 3D SHG imaging of the inner and outer surfaces of the aortic wall was performed using a commercial multiphoton microscope (A1R-MP; Nikon). Then, 11 texture feature parameters, including the correlation, contrast, entropy, energy, sum mean, variance, homogeneity, cluster shade, cluster prominence, max probability, and inverse variance, of the aortic collagen fibers were extracted from the 3D SHG image stacks using the 3D GLCM algorithm (Fig. 1). Finally, statistical analysis based on one-way ANOVA and Tukey's multiple comparison test was performed using GraphPad Prism software to sift out aging-associated features.

Results and Discussions By comparing the SHG images of the WKY rats of different ages, we found that the aortic collagen fibers gradually became thicker, less dense, and more evenly distributed from 3 w to 12 w and 44 w (Figs. 2 and 3), regardless of the intima, media, or adventitia. However, the general morphology of the collagen fibers in the aortic intima and media was remarkably different from that in the aortic adventitia. The intima and media collagen fibers were relatively straight (Fig. 2), whereas the adventitial collagen fibers were arranged in curved bundles and had stronger SHG signals (Fig. 3). The 3D GLCM analysis and statistics of the aforementioned SHG images further showed that in the aortic intima and media, six texture features of the collagen fibers, including the correlation, contrast, entropy, sum mean, variance, and homogeneity, were significantly different among the

three age groups. These features characterized the consistency, clarity, strength heterogeneity, overall strength, strength concentration, and structural isotropy of the fiber textures (Fig. 4). Similarly, for the adventitial layers, three aging-associated textural features—the sum mean, variance, and homogeneity—were sifted out (Fig. 5). The age-related changes revealed by these preferential texture features were generally consistent with those observed in the 3D SHG image stacks. These results demonstrated that combining SHG imaging with the 3D GLCM algorithm is a practical strategy for assessing aging-related changes in the collagen fibers in the aortic wall, and that 3D GLCM texture features such as the correlation, contrast, entropy, sum mean, variance, and homogeneity are promising quantitative indicators of aorta aging.

Conclusions This study proposed a novel strategy that combined SHG imaging with 3D GLCM for aortic-aging assessment from the fresh perspective of the collagen fiber microstructure. The collagen fibers within the aortic intima-media and adventitia of WKY rats with different weeks of age were imaged using SHG microscopy. The 3D GLCM was then used to quantify the stere omicrostructural characteristics of the collagen fibers based on the 3D SHG image stacks, and a variety of aging-related texture features, including the correlation, contrast, entropy, sum mean, variance, and homogeneity, were sifted out. The proposed method and derived texture features are expected to provide a powerful tool and important reference indicators for assessing the degree of vascular aging. Moreover, this method may benefit the research on age-related cardiovascular diseases. Nevertheless, it should be noted that the SHG intensity was highly dependent on the overlap of the laser polarization with the fiber alignment. The excitation light used in this study was linearly polarized. The intensity of the SHG signal appeared to be at a maximum when the laser polarization direction was parallel to the orientation of the collagen fibers, whereas it appeared at a minimum when the two directions were perpendicular. We hope to consider laser polarization in our future studies, despite a variety of measures taken to minimize the effects of polarization on the quantitative analysis results of the SHG images in the present study. In addition, we found that the three age groups considered in this study could not be completely distinguished from each other by relying merely on a single 3D GLCM texture feature, although the 3D GLCM algorithm is considered highly sensitive to fiber microstructures. Therefore, more sensitive and valuable quantitative analytical methods merit further investigation.

Key words medical optics; second harmonic generation microscopy; three-dimensional gray level co-occurrence matrix; aorta; aging-related changes; collagen fibers